JOURNAL OF SOLID STATE CHEMISTRY 84, 365–374 (1990)

A Novel Niobium Phosphate Bronze with a Tunnel Structure, $K_3Nb_6P_4O_{26}$, Member $n = \infty$ of the Series $(K_3Nb_6P_4O_{26})n \cdot KNb_2PO_8$

A. BENABBAS, M. M. BOREL, A. GRANDIN, A. LECLAIRE, AND B. RAVEAU

Laboratoire CRISMAT—ISMRa, Université de Caen, Bd du Maréchal Juin, 14032 Caen Cedex, France

Received June 15, 1989; in revised form October 19, 1989

A new niobium phosphate bronze with a tunnel structure $K_3Nb_6P_4O_{26}$ has been synthesized and its structure has been determined from a single crystal by X-ray diffraction. It crystallizes in the space group *Pnma* with $a = 14.7484(9)$ Å, $b = 31.582(2)$ Å, $c = 9.3859(6)$ Å. Its structure consists of $[Nb_3P_2O_{13}]_\infty$ layers sharing the corners of their NbO_6 octahedra and PO_4 tetrahedra. The geometry of those layers derives from the hexagonal tungsten bronze and is compared to that of $K_7Nb_{14}P_9O_{60}$. This oxide represents the member $n = \infty$ of the structural family $(K_3Nb_6P_4O_{26})_n \cdot KNb_2PO_8$, whereas $K_7Nb_{14}P_9O_{60}$ previously described corresponds to $n = 2$.

The exploration of *A*–P–W–O systems in which *A* is an alkaline or alkaline earth cation has allowed a large family of anisotropic metal-like phases, called phosphate tungsten bronzes, to be synthesized (*1*). A very original study of the intercalation of cations in those phases and of their electron transport properties has been performed by Wang and Greenblatt (*2*) which shows a very promising field for research from a fundamental as well as from an applied point of view. The fact that such properties are due to the mixed valence of tungsten, W(V)/W(VI), suggests that several other families of phosphate bronzes of transition metals should be synthesized. Starting from this idea, the K–Nb–P–O system was recently investigated. Two new niobium phosphate bronzes with a tunnel structure were isolated: $KNb_3P_3O_{15}$ (*3*) closely related to the tetragonal tungsten bronze (TTB) described by Magneli (*4*) and $K_7Nb_{14+x}P_{9-x}O_{60}$ (*5*) related to the intergrowth tungsten bronzes (ITB) described by Hussain and Kihlborg (*6*, *7*). The latter bronze can be described as the second member of a hypothetical large family $(K_3Nb_6P_4O_{26})n \cdot KNb_2PO_8$. We report here on the synthesis and structure of the phosphate bronze $K_3Nb_6P_4O_{26}$, which corresponds to the member $n = \infty$ of this series.

Synthesis

The quantitative synthesis of powder of oxide $K_3Nb_6P_4O_{26}$ was performed in two steps. First, a stoichiometric mixture of K_2CO_3, $H(NH_4)_2PO_4$, and Nb_2O_5 was heated up to 673 K in air. In a second step the finely ground powder mixed with an appropriate amount of niobium, sealed in an evacuated silica ampoule, was heated up to 1173 K for 3 hr. The X-ray diffraction powder pattern of this phase was indexed in an

0022-4596/90 $3.00

TABLE I

$K_3Nb_6P_4O_{26}$ INTERRETICULAR DISTANCES

$h\ k\ l$	d_{obsd}	d_{calcd}	I/I_0	$h\ k\ l$	d_{obsd}	d_{calcd}	I/I_0
2 2 0	6.701	6.682	7.5	1 15 1	2.035	2.035	4.5
2 0 1	5.794	5.799	54	5 9 2		2.035	
0 0 2	4.696	4.693	13.5	6 9 1	1.969	1.968	31
3 2 1	4.195	4.198	10	6 2 3	1.918	1.919	7.5
0 4 2	4.033	4.034	3	7 1 2		1.919	
0 8 0	3.945	3.948	100	3 7 4		1.917	
2 2 2	3.837	3.840	7.5	2 9 4	1.884	1.886	5
3 0 2	3.396	3.395	75	5 8 3		1.886	
2 8 1	3.259	3.263	8	4 14 1		1.885	
4 3 1		3.263		5 11 2		1.884	
1 0 3	3.061	3.060	31.5	6 11 0	1.866	1.867	7
4 5 1	3.015	3.015	16.5	3 8 4		1.866	
2 0 3	2.879	2.880	24.5	2 1 5	1.817	1.816	6
5 0 1	2.815	2.814	50	8 3 0		1.816	
5 4 1	2.648	2.651	1.5	1 14 3		1.816	
1 6 3		2.646		8 1 1	1.806	1.806	6
3 3 3	2.564	2.560	16	1 16 2		1.806	
4 4 3	2.285	2.284	13.5	7 6 2		1.805	
5 0 3	2.144	2.146	5				
0 6 4		2.143					

orthorhombic cell, in agreement with the parameters obtained from the single crystal study (Table I).

Single crystals could be synthesized from samples of nominal composition "$KNb_2P_2O_{10}$." Their preparation was also performed in two steps. First K_2CO_3, $H(NH_4)_2PO_4$, and Nb_2O_5 were heated up to 673 K in air, in order to eliminate CO_2, H_2O, and NH_3. In the second step, the finely ground product was mixed with an appropriate amount of niobium and sealed in an evacuated silica ampoule. This sample was then heated up to 1373 K for about 1 month. In this condition, black needles could be isolated from the mixture, whose composition deduced from the structural determination $K_3Nb_6P_4O_{26}$ was confirmed by microprobe analysis.

Structure Determination

A dark crystal with dimension 0.072 × 0.048 × 0.048 mm was selected for the structure determination. The cell parameters reported in Table II were determined and refined by diffractometric techniques at 294 K with a least-squares refinement based upon 25 reflections with $18 < \theta < 22°$.

The systematic absences, $h + l = 2n + 1$ for $0kl$ and $h = 2n + 1$ for $hk0$, are consistent with the space groups *Pnma* (No. 62) and $Pn2_1a$ (other setting of $Pna2_1$ No. 33). The presence of $0v0$ Harker peaks in the Patterson function allowed the centrosymmetrical space group *Pnma* to be chosen.

The data were collected on a CAD-4 Enraf-Nonius diffractometer with the data collection parameters reported in Table II. The reflections were corrected for Lorentz and polarization effects; no absorption corrections were performed.

The atoms were located by the heavy-atom method. The small number of reflections (1674) did not allow the anisotropic thermal factors to be refined for all the atoms. Anisotropic factors were only attributed to Nb and K atoms, whereas all the

TABLE II

SUMMARY OF CRYSTAL DATA, INTENSITY MEASUREMENTS, AND STRUCTURE REFINEMENT PARAMETERS FOR $K_3Nb_6P_4O_{26}$

1. Crystal data	
Space group	*Pnma* (62)
Cell dimensions	a = 14.7484(9) Å
	b = 31.582(2) Å
	c = 9.3859(6) Å
Volume	V = 4371.8(8) Å^3
Z	8
2. Intensity measurement	
λ (Mo$K\alpha$)	0.71073 Å
Scan mode	$\omega - 4/3\ \theta$
Scan width (°)	1. + 0.35 tan θ
Slit aperture (mm)	1. + tan θ
Max θ (°)	45
Standard reflections	3 measured every 2000 sec (no decay)
Reflections with $I > 2.5\sigma$	1674
μ (mm^{-1})	2, 34
3. Structure solution and refinement	
Parameters refined	201
Agreement factors	R = 0.044, R_w = 0.044
Weighting scheme	$W = 1./\sigma(I)^2$

other atoms were refined with isotropic thermal factors. During the refinement some B iso of the oxygen atoms became negative and during the subsequent refinement were fixed at 0.5. The R factors and the atomic distances were not affected by fixing of some B iso factors. The atomic parameters of Table III are obtained for R = 0.044 and R_w = 0.045.[1]

Description of the Structure and Discussion

As expected from the analysis of the structure of the niobium phosphate bronze $K_7Nb_{14+x}P_{9-x}O_{60}$ (5), the host lattice "$Nb_6P_4O_{26}$" is closely related to that structure, and can be considered as the extreme member $n = \infty$ of the series $(K_3Nb_6P_4O_{26})_n \cdot KNb_2PO_8$. The projection of the structure of this phase on to (010) (Fig. 1a) shows that its $[Nb_3P_2O_{13}]_\infty$ layers exhibit a great similarity with the (100) layers observed for $K_7Nb_{14+x}P_{9-x}O_{60}$ (Fig. 1c). One indeed recognizes in both cases infinite chains of corner-sharing NbO_6 octahedra running along **c** for $K_3Nb_6P_4O_{26}$ and along **b** for $K_7Nb_{14}P_9O_{60}$ connected through PO_4 tetrahedra and forming six-sided rings which derive from the hexagonal tungsten bronze (HTB) rings (Fig. 1d) by replacing two octahedra out of six by PO_4 tetrahedra. However, the geometry of the octahedral chains running along **c** is fundamentally different in both structures. One can indeed characterize those chains by three O–O–O angles

[1] List of structure factors and anisotropic thermal motion parameters are available upon request from the authors.

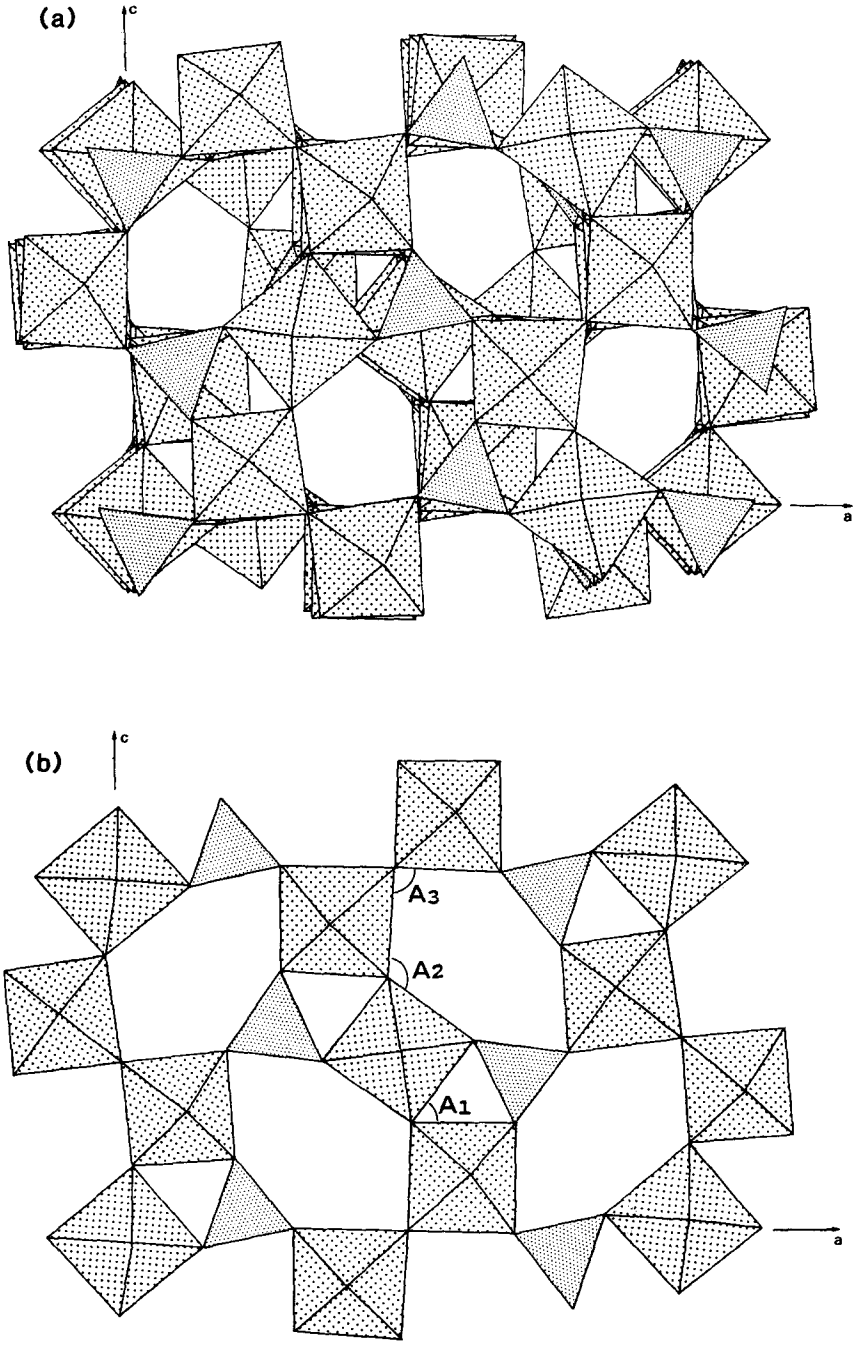

FIG. 1. (a) Projection of $K_3Nb_6P_4O_{26}$ onto (010) and layers of six-sided rings in (b) $K_3Nb_6P_4O_{26}$, (c) $K_7Nb_{14}P_9O_{60}$ and (d) hexagonal tungsten bronze.

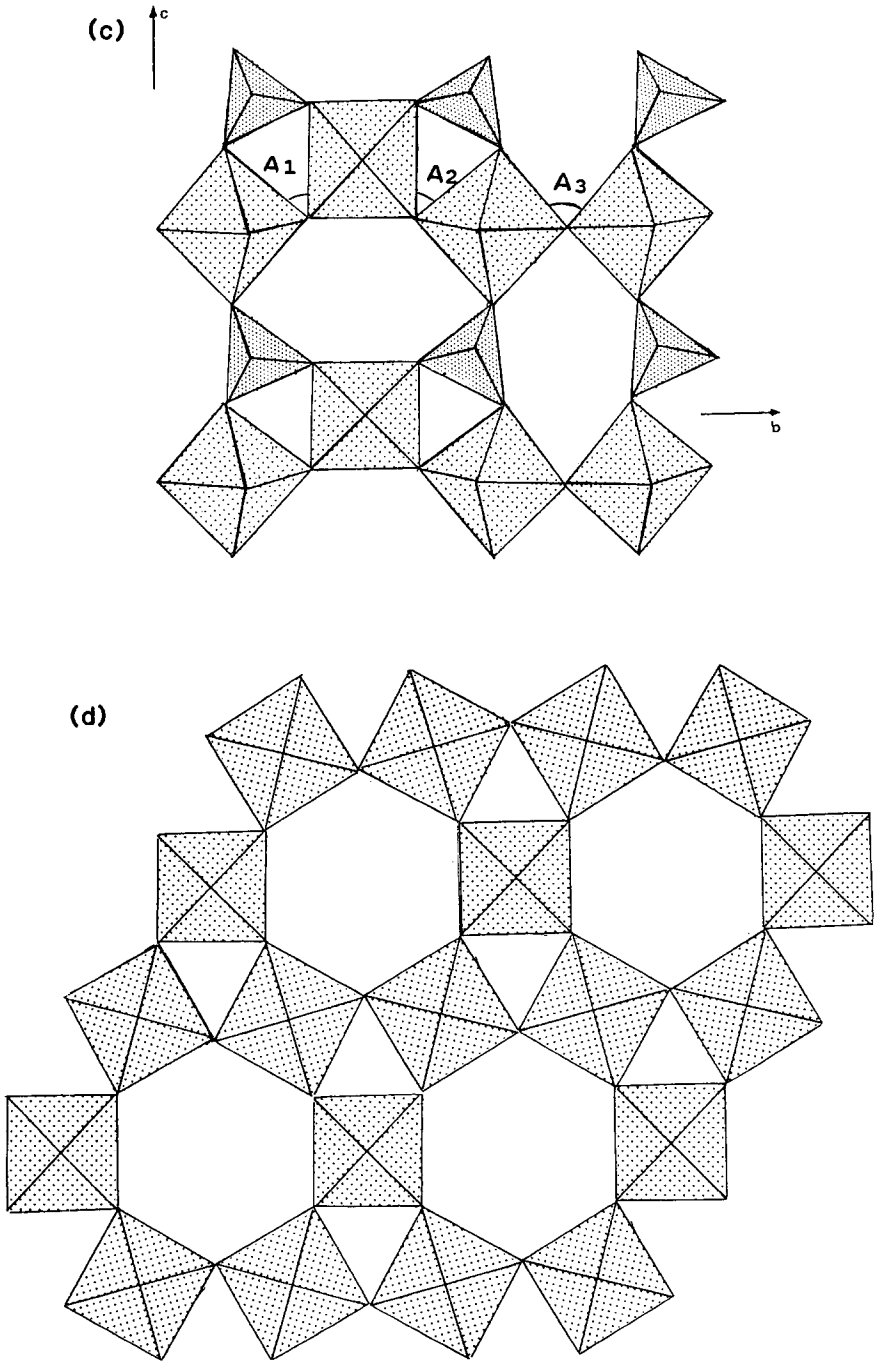

FIG. 1—*Continued*

TABLE III

POSITIONAL PARAMETERS AND THEIR ESTIMATED STANDARD DEVIATIONS

Atom	x	y	z	B(A2)
Nb(1)	0.0996(1)	0.69040(7)	0.3636(2)	0.51(2)
Nb(2)	0.0896(1)	0.56795(6)	0.3625(2)	0.37(2)
Nb(3)	0.0996(1)	0.44548(5)	0.3684(2)	0.31(2)
Nb(4)	0.2049(1)	0.69011(7)	0.0066(2)	0.43(2)
Nb(5)	0.2904(1)	0.69061(7)	0.6324(2)	0.28(2)
Nb(6)	0.5079(1)	0.44003(6)	0.5014(3)	0.37(2)
K(1)	0.3676(7)	0.750	0.248(1)	2.2(2)
K(2)	0.4636(9)	0.0250	0.250(1)	3.3(2)
K(3)	0.0963(6)	0.6240(2)	0.7248(7)	2.9(1)
K(4)	0.3348(5)	0.5032(2)	0.2525(7)	2.5(1)
P(1)	0.4868(4)	0.6714(2)	0.4470(6)	0.31(7)*
P(2)	0.0853(4)	0.3320(2)	0.4201(5)	0.29(7)*
P(3)	0.2190(4)	0.4200(2)	0.0779(6)	0.38(7)*
P(4)	0.2076(4)	0.5792(2)	0.0567(5)	0.32(7)*
O(1)	0.069(1)	0.750	0.354(2)	0.5*
O(2)	−0.003(1)	0.6789(5)	0.213(2)	1.0(3)*
O(3)	0.0057(9)	0.6869(5)	0.528(1)	0.6(2)*
O(4)	0.1924(9)	0.6973(5)	0.497(2)	1.0(2)*
O(5)	0.183(1)	0.6946(5)	0.209(2)	0.9(2)*
O(6)	0.098(1)	0.6253(5)	0.385(1)	0.5*
O(7)	0.010(1)	0.5641(4)	0.208(2)	0.6(2)*
O(8)	−0.001(1)	0.5520(4)	0.499(2)	0.4(2)*
O(9)	0.1901(9)	0.5647(4)	0.526(1)	0.5*
O(10)	0.1956(9)	0.5697(5)	0.217(1)	0.3(2)*
O(11)	0.114(1)	0.5020(5)	0.351(2)	0.8(2)*
O(12)	0.0241(9)	0.4355(4)	0.203(1)	0.2(2)*
O(13)	0.200(1)	0.4423(5)	0.517(2)	1.0(2)*
O(14)	0.2107(9)	0.4354(4)	0.229(1)	0.4(2)*
O(15)	0.088(1)	0.3798(4)	0.417(1)	0.5*
O(16)	0.213(2)	0.750	−0.008(3)	1.2(3)*
O(17)	0.0692(8)	0.6925(6)	−0.029(1)	0.5(2)*
O(18)	0.3388(8)	0.6873(5)	0.023(1)	0.5*
O(19)	0.218(1)	0.6821(4)	−0.206(1)	0.7(2)*
O(20)	0.209(1)	0.6259(5)	0.022(2)	0.9(2)*
O(21)	0.299(1)	0.750	0.647(2)	0.5(3)*
O(22)	0.397(1)	0.6854(6)	0.766(2)	1.3(2)*
O(23)	0.3998(9)	0.6947(4)	0.488(1)	0.5*
O(24)	0.285(1)	0.6272(6)	0.575(2)	1.2(2)*
O(25)	0.500	0.500	0.500	0.9(3)*
O(26)	0.371(1)	0.4409(5)	0.476(2)	0.7(2)*
O(27)	0.6473(9)	0.4396(4)	0.520(2)	0.6(2)*
O(28)	0.514(1)	0.3755(5)	0.509(2)	0.8(2)*

Note. Atoms marked with asterisks were refined isotropically. Anisotropically refined atoms are given in the form of the isotropic equivalent displacement parameter defined as $(4/3) \times [a2 \times B(1,1) + b2 \times B(2,2) + c2 \times B(3,3) + ab(\cos\gamma) \times B(1,2) + ac(\cos\beta) \times B(1,3) + bc(\cos\alpha) \times B(2,3)]$.

labeled A_1, A_2, and A_3, formed by the edges of the octahedra (Figs. 1b and 1c). Thus, it is observed for the sequence "A_1, A_2, A_3" that if A_1 and A_3 are equal to 60 and 90° in both structures, respectively, A_2 = 60° for $K_7Nb_{14}P_9O_{60}$ (Fig. 1c) against 120° for $K_3Nb_6P_4O_{26}$ (Fig. 1b). Consequently only one sort of hexagonal tunnel running along **b** is observed in $K_3Nb_6P_4O_{26}$ (Fig. 1a) against two sorts of tunnels for $K_7Nb_{14}P_9O_{60}$, called HTB and BMT owing to their similarity with hexagonal tungsten bronze and hexagonal brownmillerite (BMT) tunnels, respectively. Clearly from this analysis, it appears that the geometry of the hexagonal tunnels of $K_3Nb_6P_4O_{26}$, characterized by two O–O–O angles of 90°, is rather different from that of the HTB tunnels (Fig. 1d) and that the absence of BMT tunnels along that direction prevents this extreme member from being closely related to the ITB structure.

TABLE IV

DISTANCES (Å) AND ANGLES (°) IN THE PO_4 TETRAHEDRA

P(1)	O(2^{iv})	O(17^{iv})	O(23)	O(28^{x})
O(2^{iv})	1.53(2)	2.55(2)	2.43(3)	2.58(3)
O(17^{iv})	110(1)	1.59(2)	2.53(2)	2.50(3)
O(23)	105(1)	108.4(9)	1.53(2)	2.56(2)
O(28^{x})	114(1)	106(1)	113(1)	1.54(2)
P(2)	**O(3^{i})**	**O(15)**	**O(18^{iii})**	**O(22^{viii})**
O(3^{i})	1.55(2)	2.57(3)	2.51(2)	2.51(2)
O(15)	114(1)	1.51(2)	2.58(2)	2.51(2)
O(18^{iii})	106(1)	112(1)	1.60(2)	2.56(2)
O(22^{viii})	107(1)	109(1)	108(1)	1.57(2)
P(3)	**O(9^{viii})**	**O(14)**	**O(24^{viii})**	**O(27^{xii})**
O(9^{viii})	1.51(2)	2.41(3)	2.47(3)	2.44(3)
O(14)	106(1)	1.51(2)	2.45(3)	2.52(2)
O(24^{viii})	111(1)	109(1)	1.49(2)	2.50(3)
O(27^{xii})	107(1)	112(1)	111(1)	1.53(2)
P(4)	**O(10)**	**O(13^{viii})**	**O(20)**	**O(26^{viii})**
O(10)	1.55(2)	2.45(3)	2.56(3)	2.49(3)
O(13^{viii})	104(1)	1.56(2)	2.53(3)	2.54(3)
O(20)	114(1)	111(1)	1.51(2)	2.45(3)
O(26^{viii})	109(1)	111(1)	108(1)	1.52(2)

Note. Symmetry code: *i*: $-x$; $1-y$; $1-z$. *ii*: x; y; $1+z$. *iii*: $\frac{1}{2}-x$; $1-y$; $\frac{1}{2}+z$. *iv*: $\frac{1}{2}+x$; y; $\frac{1}{2}-z$. *v*: $\frac{1}{2}+x$; $\frac{3}{2}-y$; $\frac{1}{2}-z$. *vi*: x; $\frac{3}{2}-y$; z. *vii*: $\frac{1}{2}-x$; $y-\frac{1}{2}$; $z-\frac{1}{2}$. *viii*: $\frac{1}{2}-x$; $1-y$; $z-\frac{1}{2}$. *ix*: $\frac{1}{2}-x$; $y-\frac{1}{2}$; $\frac{1}{2}+z$. *x*: $1-x$; $1-y$; $1-z$. *xi*: $1-x$; $y-\frac{1}{2}$; $1-z$. *xii*: $x+\frac{1}{2}$; y; $\frac{1}{2}-z$.

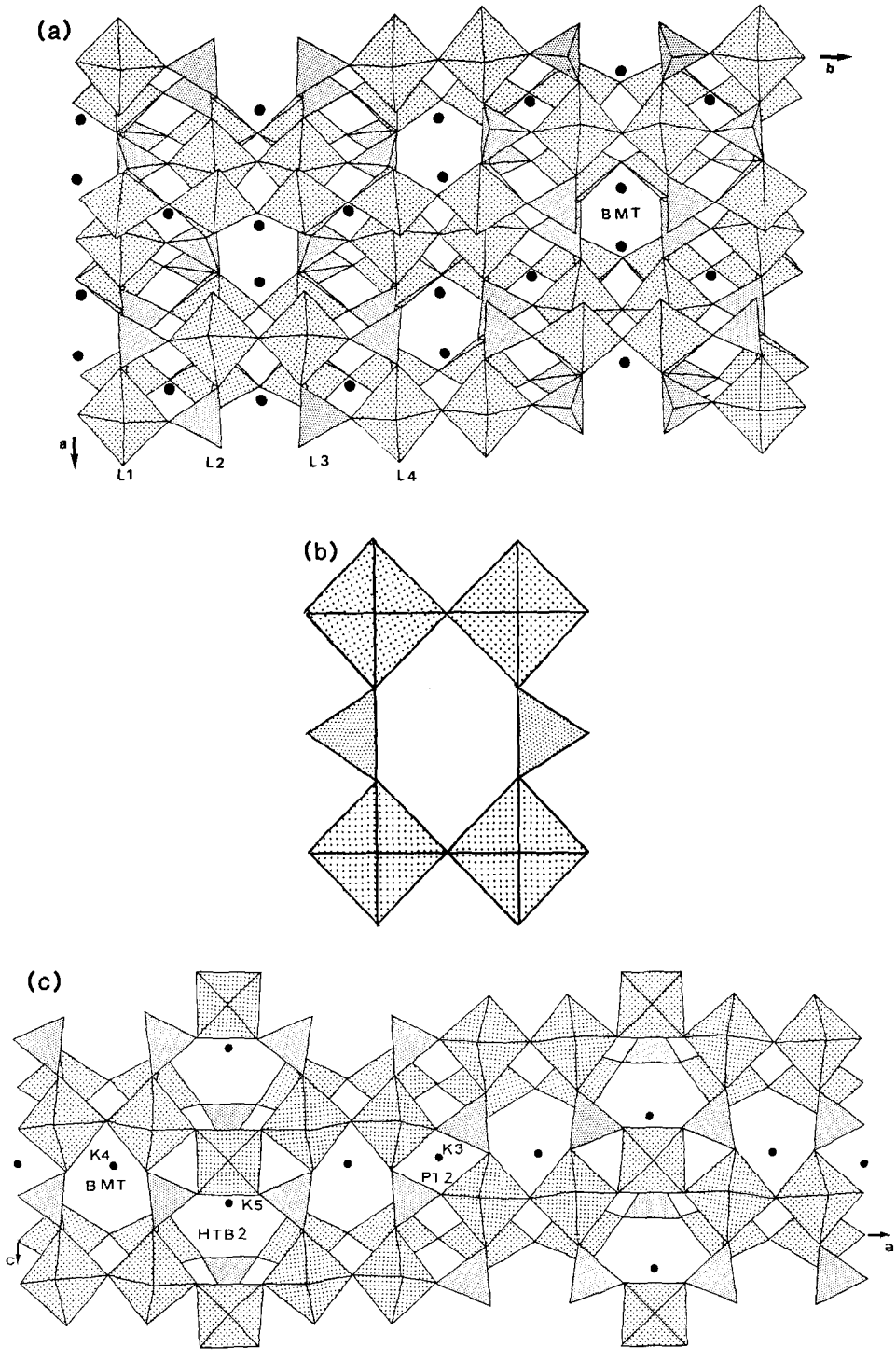

FIG. 2. (a) Projection along c of $K_3Nb_6P_4O_{26}$ showing brownmillerite-type tunnels. (b) Ring of two groups of two octahedra connected through PO_4 tetrahedra. (c) Projection along b of $K_7Nb_{14}P_9O_{60}$ showing brownmillerite-type tunnels.

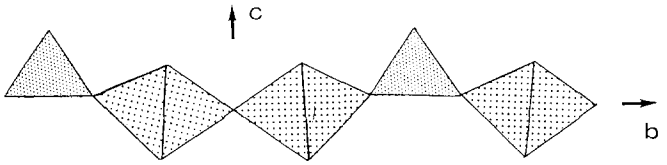

FIG. 3. The $[Nb_2PO_8]_\infty$ chains.

The view of the structure of this phase along **c** (Fig. 2a) shows that the "$Nb_6P_4O_{26}$" framework results from the stacking of identical $[Nb_3P_2O_{13}]_\infty$ layers by sharing the corners of their polyhedra. Two successive layers, labeled L1 and L2, share the corners of their PO_4 tetrahedra with those of the NbO_6 octahedra so that L2 is deduced from L1 by rotation around a binary axis parallel to **c**. The identical L2 and L3 layers share only the corners of their octahedra and deduced one from the other by a mirror. L3 and L4 are connected in the same way as L1 and L2. The complete stacking of the cell is obtained by the assemblage of (2×4) $[Nb_3P_2O_{13}]_\infty$ layers. From this view along **c**, it can be seen that this framework delimits hexagonal tunnels similar to those encountered in the brownmillerite running along **c** (Fig. 2a). These BMT tunnels, formed of rings themselves built up of two groups of two octahedra connected through single PO_4 tetrahedra (Fig. 2b), are absolutely similar to those running along **b** in $K_7Nb_{14}P_9O_{60}$ (Fig. 2c). The comparison of the two projections (Figs. 2a and 2c) shows that $K_3Nb_6P_4O_{26}$ differs from $K_7Nb_{14}P_9O_{60}$ by the absence of $[Nb_3P_2O_{13}]_\infty$ chains which run along **b** in the latter structure (Fig. 3). Thus, it seems that the presence of those chains imposes the different geometry of the $[Nb_3P_2O_{13}]_\infty$ layers observed in $K_7Nb_{14}P_9O_{60}$.

The view of this structure along **a** (Fig. 4) shows its similarity with the perovskite; one indeed observes four-sided small tunnels running along **a**, and ReO_3-type strings of six octahedra running along **b**. The latter octahedral strings share the corners of two of their octahedra forming infinite chains running along **b** (Fig. 5).

A remarkable feature of this structure concerns the distortion of its polyhedra. The PO_4 tetrahedra are not so regular as in $K_7Nb_{14}P_9O_{60}$ and in a general way as in other monophosphates. The P–O distances

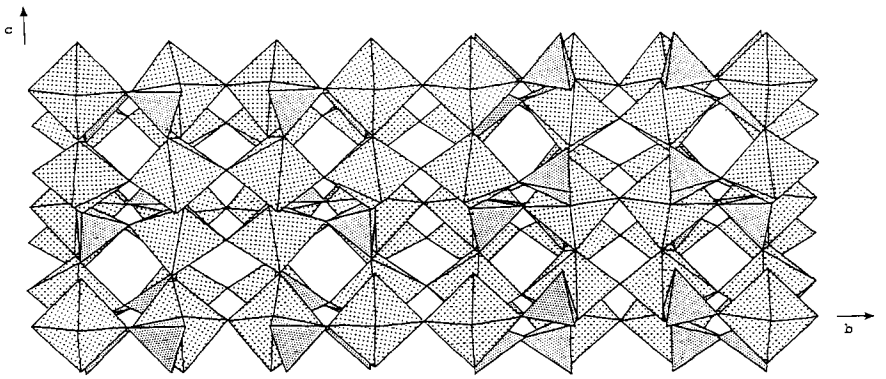

FIG. 4. Projection along *a* of the $K_3Nb_6P_4O_{26}$ structure.

TABLE V

DISTANCES (Å) AND ANGLES (°) IN THE NbO_6 OCTAHEDRA

Nb(1)	O(1)	O(2)	O(3)	O(4)	O(5)	O(6)
O(1)	1.938(6)	2.81(2)	2.74(3)	2.81(3)	2.78(3)	3.97(3)
O(2)	88.2(9)	2.10(2)	2.97(2)	3.96(3)	2.78(3)	2.77(3)
O(3)	86.0(9)	90.8(7)	2.08(2)	2.79(2)	3.98(3)	2.72(3)
O(4)	95.3(10)	176.6(8)	89.8(8)	1.87(2)	2.70(3)	2.87(3)
O(5)	92.8(10)	87.9(8)	178.2(8)	91.6(8)	1.90(2)	3.02(3)
O(6)	165.3(9)	83.3(7)	82.2(8)	93.4(8)	98.9(8)	2.07(2)
Nb(2)	O(6)	O(7)	O(8)	O(9)	O(10)	O(11)
O(6)	1.83(2)	2.86(3)	2.94(2)	2.70(3)	2.77(3)	3.91(3)
O(7)	101.3(8)	1.87(2)	2.76(3)	3.99(3)	2.74(3)	2.83(3)
O(8)	103.0(8)	93.7(8)	1.92(2)	2.86(3)	3.97(3)	2.71(3)
O(9)	85.3(7)	171.8(8)	89.5(8)	2.14(2)	2.90(2)	2.80(3)
O(10)	90.1(8)	88.0(8)	166.1(8)	87.1(6)	2.08(2)	2.76(3)
O(11)	165.9(8)	90.3(8)	84.0(7)	82.5(7)	82.2(8)	2.12(2)
Nb(3)	O(8^{i})	O(11)	O(12)	O(13)	O(14)	O(15)
O(8^{i})	1.91(2)	2.77(2)	2.84(3)	2.95(3)	4.02(3)	2.62(2)
O(11)	96.2(8)	1.81(2)	2.85(2)	2.76(3)	2.79(2)	3.93(3)
O(12)	95.3(8)	99.1(8)	1.94(2)	3.94(3)	2.76(3)	2.83(2)
O(13)	96.4(9)	91.3(8)	163.4(8)	2.04(2)	2.72(2)	2.75(3)
O(14)	173.4(7)	90.1(8)	85.7(8)	81.4(7)	2.12(2)	3.08(2)
O(15)	80.8(7)	172.6(8)	88.0(7)	82.3(7)	92.7(7)	2.13(2)
Nb(4)	O(5)	O(16)	O(17)	O(18)	O(19)	O(20)
O(5)	1.94(2)	2.73(3)	2.80(2)	2.90(2)	3.96(3)	2.82(3)
O(16)	91(1)	1.901(5)	2.81(3)	2.73(3)	2.84(3)	3.93(3)
O(17)	89.7(7)	91(1)	2.03(1)	4.01(3)	2.78(2)	2.98(3)
O(18)	95.5(7)	89(1)	174.8(6)	1.98(2)	2.79(2)	2.72(3)
O(19)	175.1(8)	93(1)	86.4(7)	88.4(6)	2.02(2)	2.79(3)
O(20)	90.5(8)	174.5(8)	94.4(8)	85.4(8)	86.7(7)	2.03(2)
Nb(5)	O(4)	O(19^{ii})	O(21)	O(22)	O(23)	O(24)
O(4)	1.95(2)	2.85(3)	2.69(3)	3.96(3)	3.06(2)	2.71(3)
O(19^{ii})	97.2(8)	1.87(2)	2.81(2)	2.65(3)	3.94(3)	2.86(3)
O(21)	90(1)	97.1(9)	1.886(4)	2.73(3)	2.73(2)	3.94(3)
O(22)	176.6(8)	86.0(8)	89(1)	2.02(2)	2.62(2)	3.05(3)
O(23)	98.2(7)	164.3(7)	86.1(9)	78.7(6)	2.11(2)	2.84(3)
O(24)	84.7(8)	92.9(7)	169(1)	96.3(8)	85.6(7)	2.07(2)
Nb(6)	O(7^{iii})	O(12^{iv})	O(25)	O(26)	O(27)	O(28)
O(7^{iii})	1.96(2)	3.89(3)	2.82(2)	2.81(3)	2.92(3)	2.70(3)
O(12^{iv})	171.9(8)	1.94(2)	2.81(2)	2.82(2)	2.77(2)	2.75(3)
O(25)	93.7(6)	94.3(5)	1.898(3)	2.68(2)	2.90(2)	3.94(3)
O(26)	89.0(8)	90.4(8)	85.7(5)	2.04(2)	4.10(3)	2.97(3)
O(27)	92.9(8)	87.7(7)	93.9(5)	178.1(9)	2.06(2)	2.82(2)
O(28)	84.6(8)	87.4(8)	178.1(6)	93.5(7)	87.0(7)	2.04(2)

Note. See Table IV for symmetry code.

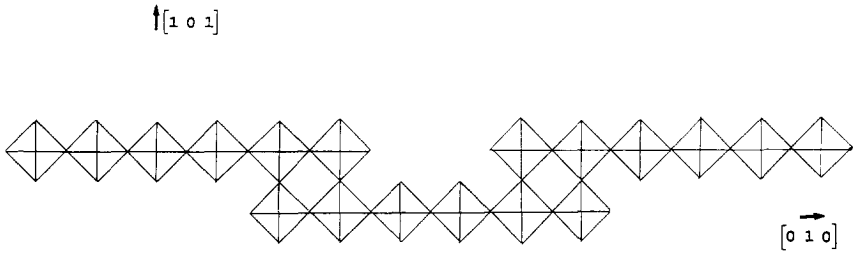

FIG. 5. Infinite chain of corner-sharing octahedra running along *b*.

range indeed from 1.491 to 1.597 Å (Table IV). Nevertheless the "O_4" tetrahedra are almost regular. In the same way the NbO_6 octahedra are very distorted with O–Nb–O angles ranging from 82.2 to 103° and O–O distances ranging from 2.62 to 3.05 Å. The NbO_6 octahedra present three Nb–O distances shorter than 2 Å and three longer ones (Table V). The Nb–O distances involving an oxygen atom common to two Nb atoms are generally shorter than those participating to the Nb–O–P bonds in agreement with the bond valence theory developed by Brown and Wu (*8*). Nevertheless some exceptions appear for the three following bonds: Nb(4)–O(19), Nb(2)–O(6), and Nb(2)–O(11) which are greater than 2 Å.

The great ability of niobium to form phosphate bronzes with a tunnel structure is confirmed by this study. A large structural family of microphases of general formula $(K_3Nb_6P_4O_{26})_n \cdot KNb_2PO_8$, should now be considered, in which $K_3Nb_6P_4O_{26}$ and $K_7Nb_{14}P_9O_{60}$ represent the members $n = \infty$ and $n = 2$, respectively. The great similarity of those oxides with the tungsten bronzes suggests that similar oxides involving rudidium, sodium, cesium, and thallium, instead of potassium, should be synthesized.

References

1. B. RAVEAU, *Proc. Indian Acad. Sci. Chem. Sci.* **96,** 419 (1986).
2. E. WANG AND M. GREENBLATT, *J. Solid State Chem.* **76,** 340 (1988).
3. A. LECLAIRE, M. M. BOREL, A. GRANDIN, AND B. RAVEAU, *J. Solid State Chem.* **80,** 12 (1989).
4. A. MAGNELI, *Arh. Kemi.* **1,** 269 (1949).
5. A. LECLAIRE, A. BENABBAS, M. M. BOREL, A. GRANDIN, AND B. RAVEAU, *J. Solid State Chem.*, in press.
6. A. HUSSAIN AND L. KIHLBORG, *Acta Crystallogr. A* **32,** 551 (1976).
7. A. HUSSAIN, *Chem. Scr.* **11,** 224 (1977).
8. I. D. BROWN, AND K. K. WU, *Acta Crystallogr. B* **32,** 1957 (1976).